Review of Chaos Detection Techniques Performed on Chaotic Maps and Systems in Image Encryption

Article *in* SN Computer Science · September 2021

DOI: 10.1007/s42979-021-00778-3

2 authors:

Joan S Muthu
SRM Institute of Science and Technology

Murali Packirisamy
SRM Institute of Science and Technology

SN Computer Science (2021) 2:392
https://doi.org/10.1007/s42979-021-00778-3

SURVEY ARTICLE

Review of Chaos Detection Techniques Performed on Chaotic Maps and Systems in Image Encryption

Joan S. Muthu[1] · P. Murali[1]

Received: 4 December 2020 / Accepted: 13 July 2021

Abstract
The security concern in recent times has been rising exponentially, this has lead for highly secured image transmission. Chaos-based image encryption is increasingly used to protect images with high degree of security than other encryption techniques. Hence, novel chaotic dynamical systems are developed for this purpose with more advanced features and models. Various chaos detection techniques are performed on them to examine and measure their complexity. This paper analyzes the frequency of the chaos tests performed on 25 discrete chaotic maps and 18 continuous chaotic systems and reviewed for their effectiveness. It is observed that the bifurcation diagram and Lyapunov exponent are the most highly used tests for chaotic maps. Whereas, phase portrait and bifurcation diagram are commonly used for chaotic systems. Tests such as 0–1 test, three-state test and some entropy tests are seldom used. Further, the dynamics of the chaotic systems are better studied than the chaotic maps. But in most cases of chaotic maps, the test is performed only for certain random control parameter range, and its dynamics beyond that range is unknown. Hence, it is crucial to realize three important facts. First, a complete examination of the novel system must be performed with the appropriate chaos detection technique. Second, the complete range of the chaotic and non-chaotic region of a system must be presented. Third, the strength of chaos must be examined. These results are essential for generating a highly secured nonlinear key for an encryption algorithm, which makes it resistant to various attacks.

Keywords Chaos · Chaos detection techniques · Image encryption · Security

Introduction

Importance of Chaos Detection

Improvement in technology has accelerated the sharing of images in essential sectors such as health care, defense, military, e-commerce, social media, and IoT devices. Securing the images during its transmission is critical, as the cyber threats have been plaguing the internet. Many experiments and research are garnered in cryptosystem, and continuous and dynamic progress is made to shield the multimedia data from the ever continuous cyber threats and attacks.

✉ Joan S. Muthu
joans@srmist.edu.in

P. Murali
muralip@srmist.edu.in

[1] Department of Computer Science and Engineering, SRM Institute of Science and Technology, Chengalpattu District, Kattankulathur, Tamil Nadu 603203, India

Traditional encryption algorithms cannot be applied to secure the images, since there is high redundancy and strong correlation among the pixels with high data volume in images [1]. Hence, images are secured with an image encryption algorithm, where the plain image is changed to a blurred image, which is called the encrypted image. The original image is recovered by the intended receiver and is nearly impossible for a third party. Image encryption primarily consists of two steps, which are confusion and diffusion. In the confusion step, the pixel values are shuffled, keeping the pixel values intact. This reduces the correlation between the neighboring pixels. Whereas, in the diffusion step, the pixel values are changed, which reduces the relation between the plain text and the encrypted image [2].

In recent years, chaos-based image cryptosystem has gained immense attention in multimedia security. Due to the remarkable nonlinear chaotic properties, the introduction of chaos in encryption has increased the strength of the cipher. The notable feature that makes it suitable for image encryption is that it is sensitive to initial conditions, i.e.,

Published online: 26 July 2021

even for a minute change in the initial parameters, a drastic change in the output is observed. Other significant properties of chaos are mixing, ergodicity, unpredictability and non-periodicity [3–5]. Furthermore, integration of techniques such as DNA [6, 7], fuzzy transform [8], butterfly network topology [9], neural network [10], and cellular automata [11] has increased the strength of encryption.

Nevertheless, the principal features of chaos are exhibited for limited or discontinuous range in most of the conventional chaotic maps or systems. To overcome this deficiency, novel maps and systems are proposed in several works to make it more suitable for the key generation of a cryptosystem. These novel dynamical systems are developed predominantly by two methods, viz., generalization and extended forms of the conventional maps and systems. Generalization of discrete maps is done by introducing extra parameters and thereby adding extra degrees of freedom. There are two methods of introducing the extra parameters in the map equations, which are scaling parameters and shaping parameters. In scaling, the parameters are introduced using additions and multiplications, whereas in shaping, the parameters are introduced using the powering function. Some maps are developed using both the methods simultaneously [12].

To analyze the dynamics of the modified chaotic maps and systems, several chaos detection techniques are used. These techniques are performed on the different facets of the control parameters and examine the resulting dynamics exhibited by the system. They reveal the presence of fixed points, behavior of the trajectories, and most importantly, the existence of chaotic and non-chaotic regime. Hence, these chaos detection techniques play a vital role in the development of the modified chaotic maps and systems.

Author's Contribution

There are numerous survey made in the field of chaos-based image cryptosystem. They focus on the different methodologies used in encrypting an image with chaos. Nevertheless, a deeper insight into these survey papers project the following research gaps:

1. These papers do not present any knowledge of the chaos detection techniques.
2. The importance of these techniques in the development of a new chaotic map or system is not concentrated.

It is perceived that comprehension of the chaos detection techniques has become crucial and a pressing concern for understanding chaos as a phenomenon in these novel chaotic maps and systems [26]. To overcome the above-stated research gaps, the following novel contributions has been made in this review paper.

1. The knowledge of the chaos detection techniques is presented, which is extremely essential for a researcher. This knowledge is highly indispensable for the complete analysis of the novel chaotic map or system.
2. This paper reviews the utilization of various chaos detection techniques on the modified chaotic maps and systems.
3. It also focusses on the compelling need for a complete analysis of a novel chaotic map or system, before it could be applied in a cryptosystem.
4. Lack of good analysis of the chaotic maps and systems will result in erroneous reports of its dynamics. This will lead to wrong projection of the chaotic and non-chaotic range, and thereby producing poor results in its applications.

Therefore, this review paper is extremely vital for researchers who are developing new chaotic systems and chaos-based cryptosystems, as this paper stresses the importance of examining the new systems with various chaos detection tests.

Article Organization

This review paper is organized as follows. "Literature Review" projects the literature review in chaos-based image cryptosystem. "Chaos and Their Properties" highlights the properties of chaos which has intensified the image encryption algorithms. A brief study of the chaos detection tests and their importance is featured in "Chaos Detection Techniques". A comprehensive list of chaotic maps and systems and their chaotic range is presented in Section "Chaotic Maps and Systems used in Image Encryption". In addition, "Discussion" discusses the frequency of the chaos detection techniques used for evaluating the nonlinear dynamic properties of the novel chaotic maps and systems in recent works. This section also examines and highlights the usage of certain tests more frequently over the others, which could lead to the failure of the detection of some important feature in the novel systems. The review paper concludes with the importance of using the apt chaos detection technique to confirm the complete chaotic behavior in the novel dynamic systems.

Literature Review

In this section, a number of survey papers in the field of chaos-based image cryptosystem are analyzed. To highlight the developments and challenges of chaos-based cryptosystem over a stretch of time, many literature studies have been carried out which are proffered in Table 1.

Table 1 Literature review of chaos-based image cryptosystem

S. no	Survey paper	Highlights
1.	Kumar et al. [13] Chapter 1: A Survey on Chaos Based Image Encryption Techniques	Survey of chaos-based image encryption techniques
		Pros and cons of chaotic maps used in image encryption
2.	Kamal et al. [13] Chapter 2: Chaotic maps for image encryption: an assessment study	Performance analysis of the chaotic map-based encryption algorithms
		Comparison of performance measures such as PSNR, NPCR, UACI, correlation coefficient, computational time and entropy
3.	Özkaynak [14]	Comparison and categorization of chaos-based image encryption
		Features of chaos-based image encryption
4.	Murugan et al. [3]	Comparison of different image encryption techniques
		Comparison of bio-crypto algorithms
		Comparison of efficient encryption algorithms based on FPGA device, throughput (Gbps) and clock frequency (MHz)
5.	Li et al. [4]	Review of image cryptanalysis published in 2018
		Features the challenges on design and analysis of image encryption schemes
6.	Movafegh et al. [5]	Results of search based on different keywords pertaining to image encryption in (2005–2018)
		Image encryption techniques
		List of some surveys on image encryption algorithms
		Performance metrics and evaluation parameters relation in image encryption analysis
		Categorization of the proposed color image encryption schemes
		Comparison of the proposed schemes
		Comparison of the studies using the proposed schemes in color image encryption in (2012–2018)
7.	Tanwar et al. [15]	Features of chaotic maps
		Comparison of encryption algorithms based on encryption techniques, imperceptibility, compression friendliness, visual degradation, speed and cryptographic security
8.	Jain et al. [16]	Comparison of image encryption techniques based on computational time, entropy, PSNR, key sensitivity, pixel sensitivity, correlation analysis, key space and histogram analysis
9.	Younes et al. [17]	Survey of different types of image encryption
10.	Kumar et al. [18]	Survey of different encryption techniques
11.	Sharma et al. [19]	Literature review on image encryption in spatial and frequency domain
12.	Srivastava et al. [20]	Review of different encryption techniques
13.	Suneja et al. [21]	Key security evaluation
		Comparison and review of chaotic maps

The survey presented in Table 1 concludes that chaos-based image encryption is the most coveted method for securing an image, because of the intrinsic properties of chaos. The authors have also demonstrated and established the strength of chaos-based cryptosystem with performance measures such as key space analysis, key sensitivity analysis, peak signal-to-noise ratio (PSNR), unified average change in intensity (UACI), statistical attack analysis, net pixel change ratio (NPCR), Information entropy and grey value difference (GVD).

Despite the extensive review tabulated in Table 1, it is evident that the survey does not suffice adequate knowledge on the novel chaotic maps and systems developed. Hence, this review paper turns the focus on the nonlinear part of the chaos-based image encryption, and reviews the novel chaotic systems proposed in several works and the chaos detection techniques used to study these systems.

Moreover, the work of Muthu et al. [22] was motivational in highlighting the need for reviewing the various chaos detection techniques. The essence of [22] was to analyze the dynamic behavior of the modified logistic map, which was claimed to possess infinite key space [23]. But, this map was examined with the bifurcation diagram and Lyapunov exponent only for a limited range of control parameter value of [0, 10]. Figure 1 shows the bifurcation diagram and Lyapunov exponent obtained in this range.

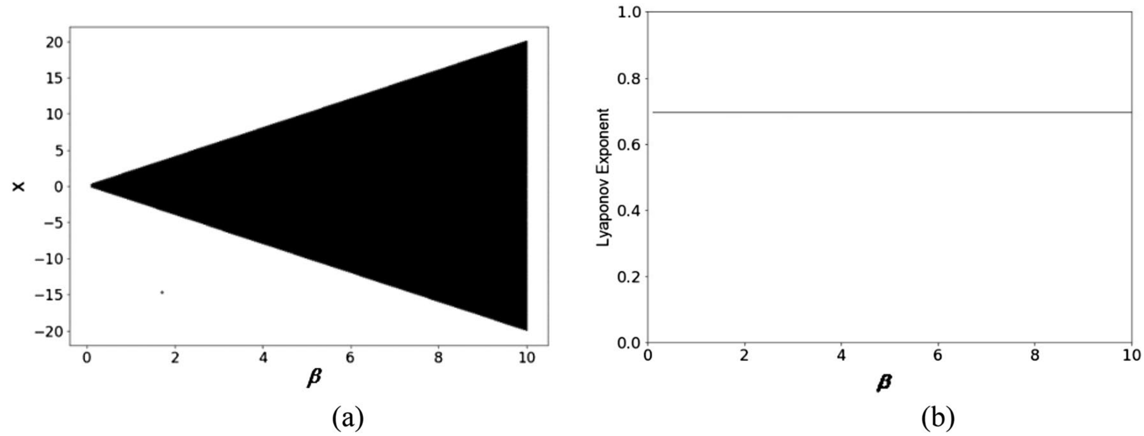

Fig. 1 Modified logistic map $\beta \in [0, 10]$. **a** Bifurcation diagram, **b** Lyapunov exponent

A deeper analysis of the modified logistic map was performed with three-state test and phase portrait apart from bifurcation diagram, Lyapunov exponent [22].

Surprisingly, a divergent dynamics of the map was observed, which is given in Fig. 2.

Figure 2 brings the dynamic nature of the modified logistic map to limelight. It shows the exhibition of the discontinuous chaotic regime of the map and hence, does not possess infinite key space [22]. This proves that the examination of the map is incomplete. Similarly, the Logistic Tent system [24] was proved to have continuous and better chaotic range

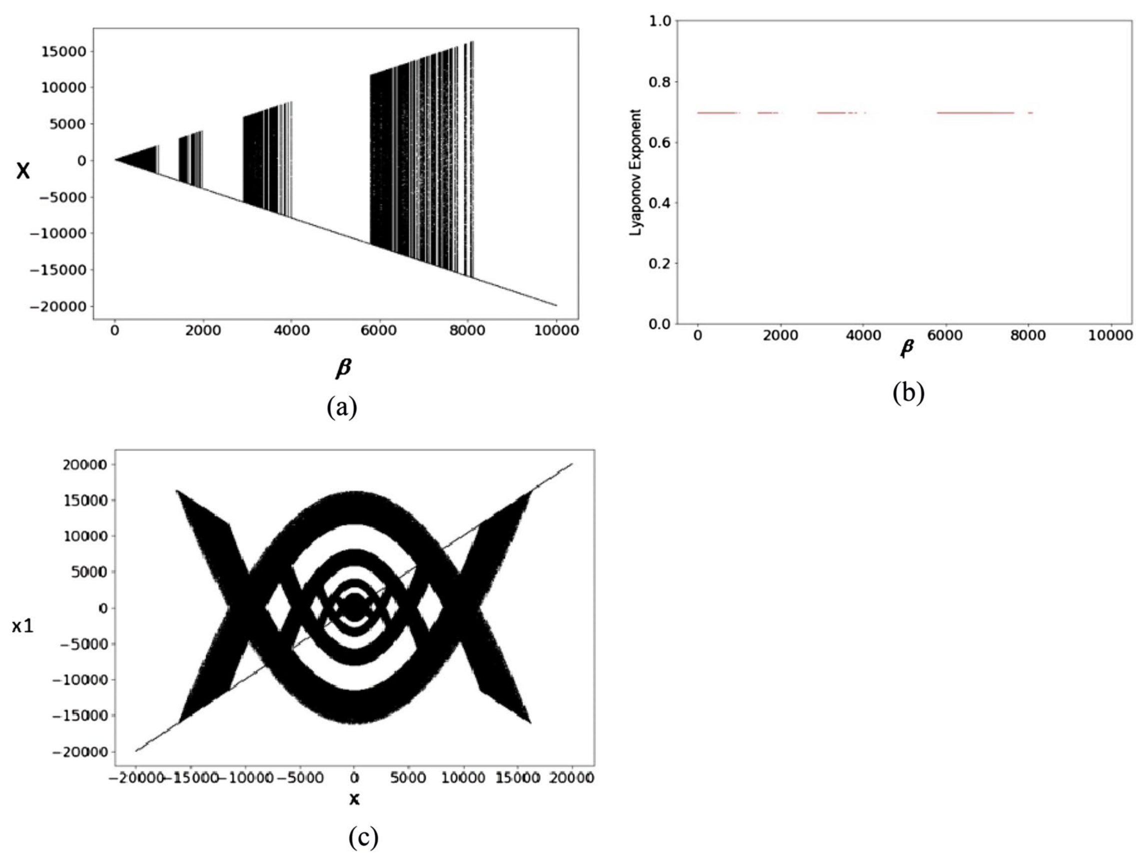

Fig. 2 Modified logistic map. **a** Bifurcation diagram for $\beta \in [0, 10000]$, **b** Lyapunov exponent for $\beta \in [0, 10000]$, and **c** phase portrait for $\beta \in [-20000, 20000]$

than the conventional chaotic maps. The authors proved the existence of chaos with the bifurcation diagram and Lyapunov exponent. But, a further examination of the Logistic Tent system using the histogram verified that its histogram distribution is not flat [25]. Hence, this result too demonstrates that the characteristic features of the novel system are not projected completely in [24].

Therefore, it is observed that the nonlinear chaotic part has been given less importance in the existing papers. Hence, this review paper focusses to overcome these research gaps.

Chaos and Their Properties

This section focusses on the different types of chaotic dynamic systems, which is elaborated in "Classification of Chaos". They have the advantage of possessing phenomenal properties which eventually makes them desirable for cryptosystems. These properties are explained in "Properties of Chaos".

Classification of Chaos

A chaotic system is defined as a physical system that is highly sensitive to initial conditions, according to physical science. But the word is associated with absolute confusion and disorder in the dictionary. Since the consequence of high sensitivity to initial conditions appears to be disordered, it is commonly associated with the dictionary meaning of chaos. However, in physical science, chaos is not random or disorder. The behavior of the system is deterministic and can be mathematically modeled. This governs the behavior of the individual step in the chaotic process. But the outcome of the combined effect of several iterations is unpredictable [27, 28]. They are defined as nonlinear dynamical systems, i.e., there is no direct relationship between the input and the outcome [29].

The chaotic process may be broadly characterized as the discrete chaotic map and the continuous system. The systems generated by the iterative formulae belong to dynamical systems with discrete time. They are labeled as chaotic maps. These maps are further classified as one-dimensional or multi-dimensional. Another class of chaotic maps are developed to overcome the limited and discontinuous range of chaotic maps, namely the coupled map lattice (CML) [30, 31]. It attributes spatiotemporal chaos [32, 33], which is nonlinear and complex in spatially extended systems. A large number of positive Lyapunov exponents of the spatiotemporal system guarantee very high randomness and ergodicity. This proves that CML is a better solution for image encryption. It is proved to be advantageous as it can be proficiently applied numerically and analytically.

In contrast to the discrete chaotic maps, the systems governed by differential equations are called as dynamical systems with continuous time. They are called the chaotic system, which is characteristic of three or higher dimensions [34]. The systems are classified as chaotic if they possess at least one positive Lyapunov exponent, and hyper-chaotic if more than one positive Lyapunov exponent is exhibited [35]. Another notable feature of a chaotic system is the strange attractor. They produce a butterfly pattern when subjected to particular values of control parameters. The strange attractors which manifest chaos are used in image encryption [34, 36].

The classifications of the chaotic nonlinear dynamical system are given in Fig. 3.

The mathematical model representing the chaotic maps and systems consists of a set of initial conditions and control

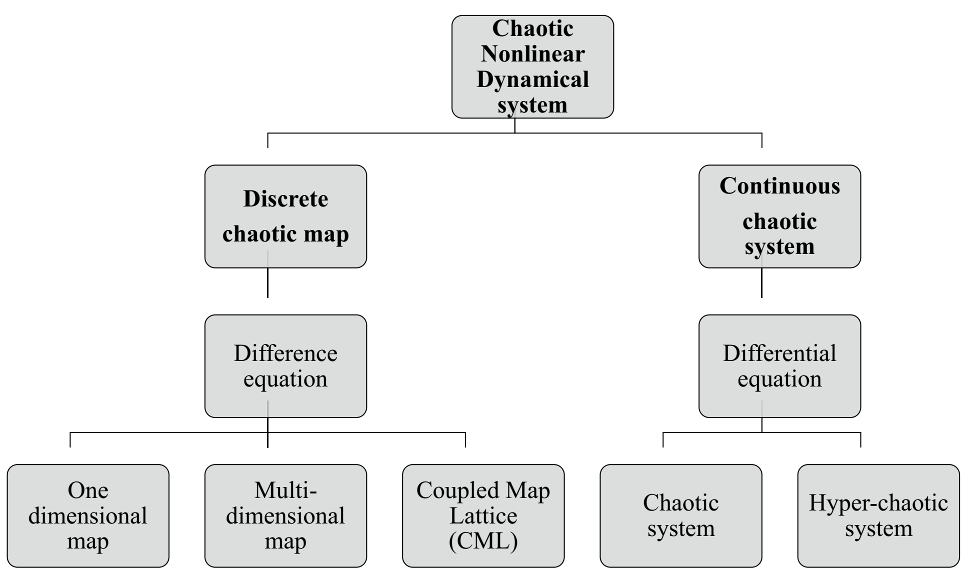

Fig. 3 Classification of chaotic nonlinear dynamical system

parameters. The chaotic process is observed to exhibit different behavior as the control parameter in the mathematical model is varied. The chaotic range of the control parameter is a crucial factor in building the key space of a cryptosystem. Furthermore, the number of dimensions of the dynamic system also influences the key space. Hence, these two factors are important concerns in determining the key space.

Properties of Chaos

Chaos is characterized by many principal properties, which makes it desirable for building a strong cryptosystem. It is identified with sensitive dependence on initial conditions, nonlinearity, deterministic, ergodicity, non-periodicity and unpredictable [11, 27, 28]. The chaos properties are summarized in Table 2.

Chaos Detection Techniques

Theorists of chaos have proposed several chaos detection techniques, which examine the behavior of the dynamic system in different dimensions [26]. They are instrumental in quantifying the complexity of the chaotic maps and systems. These chaos tests have found its significance in diverse fields such as astronomy, biology, meteorology, economics, instrumentation and social psychology. This section briefs some chaos detection techniques, with the methodology and the importance of application of these tests.

Bifurcation Diagram

Bifurcation diagram is one of the most important tool to study the behavior of the dynamic system. It is a vital graphical tool which detects the system cycles from periodic to chaotic orbits as a function of the system control parameters. It plots the control parameter of the discrete map or the continuous system verses the steady state solution. The bifurcation diagram is very significant as this plot exhibits a sudden appearance of a qualitative behavior as some parameter is varied. This behavioral change is called bifurcation and occurs at bifurcation points [12]. The bifurcation diagram is a very frequently used study method to analyze the dynamic system, as it is very simple and effortless to plot and detect the chaotic and non-chaotic regime using this diagram. It is also advantageous in detecting the period doubling route to chaos. However, its exploitation is tedious as it depends on the perceptiveness of the human vision [26].

Lyapunov Exponent

Lyapunov exponent is defined as a measure of the sensitivity and predictability of the dynamic system to changes in its initial conditions [37]. It is numerically calculated as the average logarithmic rate of separation or convergence of two nearby points of two time series Xt and Yt separated by an initial distance of $\Delta R_0 = ||X_0 - Y_0||_2$. The Lyapunov exponent is calculated with the following equation:

$$\lambda = \lim_{n\to\infty} \frac{1}{n} \sum_{i=1}^{n} \ln \left| \frac{\Delta R_i}{\Delta R_0} \right|, \tag{1}$$

where λ is the Lyapunov exponent. A dynamic system with n dimensions has n Lyapunov exponents. A system with a positive Lyapunov exponent defines it to be chaotic.

However, Lyapunov exponent has been widely used for integer-order dynamical systems, whose equation of the system is known. This approach cannot be used to examine experimental data or fractional-order dynamical system, whose equation is unknown. In such cases, phase space reconstruction must be done to calculate the Lyapunov exponent [38]. Moreover, the complexity of the computation of Lyapunov exponent increases with the increase in the number of dimension of the dynamical system [26].

0–1 Test

The 0–1 test was developed to identify regular, i.e., periodic or quasi-periodic and chaotic dynamics in deterministic dynamical systems. This test works on discretely sampled

Table 2 Chaotic properties

S. no	Chaotic properties	Meaning
1.	Sensitive to initial conditions (SIC)	A small change in the initial condition results in an exorbitant change in the output
2.	Nonlinear	The outcome does not hold a direct relationship to the input
3.	Deterministic	The process can be modeled and governed quantitatively by mathematical equations and to some extent approached quantitatively
4.	Ergodic	A long-term average prediction of the model is possible
5.	Non-periodicity	The model produces random values
6.	Unpredictable	The sequentially combined effect of many interactions results in an outcome that is unpredictable

time series data, and does not require any phase space reconstruction as in "Lyapunov exponent". This makes the test appropriate for the analysis of discrete maps, ordinary differential equations, delay differential equations, partial differential equations and real world time series [39]. Hence, the 0–1 test is used in applications where only the experiment data are available and whose equations are not known.

One-dimensional time series $\phi(n)$ for $n = 1, 2, 3,$ is the input to the test, which is used to drive the two-dimensional system given in the following equation:

$$\begin{aligned} p(n+1) &= p(n) + \phi(n)\cos cn, \\ q(n+1) &= q(n) + \phi(n)\sin cn, \end{aligned} \tag{2}$$

where $c \in (0, 2\pi)$ is fixed. The p–q plane projects bounded or Brownian-like (unbounded) trajectories. The bounded trajectories imply regular dynamics, whereas Brownian-like (unbounded) trajectories indicate chaotic dynamics.

The mean square displacement is derived with the following equation:

$$M(n) = \lim_{N\to\infty} \sum_{j=1}^{N} ([p(j+n) - p(j)]^2 + [q(j+n) - q(j)]^2. \tag{3}$$

The growth rate is calculated with the following equation, which determines the nature of the dynamic system:

$$K = \lim_{n\to\infty} \frac{\log M(n)}{\log n}. \tag{4}$$

0–1 test is a binary test, where K takes either the value $K = 0$ which signifies regular dynamics or the value $K = 1$ signifying chaotic dynamics.

The 0–1 test has many advantages over other methods for defining the dynamic behavior. The implementation is very simple and works directly with the time series data and does not require the phase space reconstruction. Further, it is also applicable to all nature of dynamical systems and dimensions. Another important advantage of 0–1 test is its caliber to identify weak chaos and its potential to discern regular behavior within noisy data. In spite of all the advantages, 0–1 test fails to distinguish between periodic and quasi-periodic orbits in a dynamic system [26].

Three-State Test (3ST)

The 3ST was developed to qualitatively diagnose the behavior of the dynamic system. It is proved to be superior to the other chaos detection tools, as it categorizes the behavior in one of the three states, viz., chaotic, quasi-periodic and periodic behaviors. Further, the detection of the period doubling route to chaos is also automated, i.e., the automation of the bifurcation diagram is achieved [26].

The 3ST depends on the analysis of pattern of the data series. The distribution of the system states is examined in the data series as a function of time. A periodic signal is distinguished with a basic pattern, which is recurrently detected in the data series at certain periods. In the case of a quasi-periodic signal, it is characterized with a basic pattern, which repeats periodically after a long observational duration. While, in a non-regular dynamics, the identification of the basic pattern is not apparent and the period cannot be defined appropriately.

In conclusion, the 3ST defines the dynamic nature of the chaotic map with the sensitivity index λ. The three states of λ are categorized with it sign, i.e., $\lambda = 0$ indicates periodical signals, $\lambda < 0$ shows the presence of quasi-periodic signals and $\lambda > 0$ identifies the chaotic signals. The 3ST establishes another important result, which is the evaluation of the period L. Thus, the 3ST yields two outputs, the cycle of periodic orbits L and the periodicity index λ, which is expressed in the following equation:

$$3ST(\phi(x)) = \left\{ \frac{L}{\lambda(n)} \right. . \tag{5}$$

Hence, besides the clear discernment of the dynamic nature of the chaotic map as periodic, quasi-periodic or chaotic, it has also confirmed other advantages. It works directly on the data series, and prior knowledge of the mathematical expression of the chaotic map is not required. It is independent of the nature of the vector field and it dimensions. Furthermore, its computational cost is low, and compared to the Lyapunov exponent and 0–1 test, the 3ST is easy to implement. Currently, the results are proved only for discrete maps, and the results for continuous time series data are yet to be established, but are promising [26].

Sample Entropy

Sample entropy (SE) is an important index to quantify the behavior of a chaotic sequence. It is used to estimate the randomness of the time series data set without any prior knowledge of dynamic system that generated the dataset [40]. It indicates the measure of the self-similarity in a sequence generated by a dynamical system. Numerous methods have been devoted for the evaluation of SE and their application in finding the regularity of the time series data is enormous [41].

The estimation of SE [42] for a time series $\{x_1, x_2, \dots, x_N\}$ of dimension N, template vector $X_m(i) = \{x_i, x_{i+1}, \dots, x_{i+m-1}\}$ of size m and acceptance tolerance r is performed in the following equation:

$$\mathrm{SE}(m, r, N) = -\log \frac{A}{B}, \tag{6}$$

where A and B are the number of vectors for $d[X_{m+1}(i), X_{m+1}(j)] < r$ and $d[X_m(i), X_m(j)] < r$, respectively, and $d\left[X_m(i), X_m(j)\right]$ represents the Chebyshev distance between $X_m(i)$ and $X_m(j)$. A higher value of SE illustrates the presence of higher irregularity, hence represents more complexity in the time series data.

Kolmogorov Entropy

The Kolmogorov entropy also known as the Kolmogorov–Sinai (KS) entropy is a measure of the predictability of a system. Kolmogorov entropy K is measured by tracking two points on the attractor with respect to time, as long as they are separated in space by less than an infinitesimally small length scale. With this method, K is obtained with high precision for a large number of pairs. For a predictable system, i.e., fully periodic, K equals zero, whereas for a stochastic system K is infinitely large. In a system featuring deterministic chaos, K is a finite positive value. Hence, KS entropy predicts the chaos and complexity of the motion in the dynamical system [37, 43].

Phase Portrait

To appreciate the complexity and dynamics of a dynamical system, it is vital to visualize its behavior in phase space. This system is defined with a set of rules that maps a state into the future. Consider a simple function f as the dynamical system, which acts on some state space U. Here, U is called the phase space. Given $f : U \rightarrow U$ and an initial point $x_0 \in U$, iterates are obtained from the following equation [44]:

$$x_{n+1} = f(x_n), \quad n \in N. \tag{7}$$

The phase portrait is obtained by plotting the x_n versus x_{n+1}, which is used to visualize both the discrete maps and the continuous systems. Nevertheless, it is more frequently used in continuous system to observe the butterfly pattern of the attractor.

Histogram

The histogram is a graphical representation of the distribution of the data series. It is a plot of the data series versus the frequency of the occurrence of the data. The histogram is an important indicator of various phenomenon in the dynamics of chaos. To understand the complexity of the dynamic system, the histogram is plotted for the phase space values generated from the dynamical system.

If the histogram shows the presence of only few values, then this indicates that the behavior of the dynamical system is regular, and the trajectories are confined to small spaces of the phase space [44]. An unequal distribution shows weak chaos, which is vulnerable to the statistical attack. An even distribution of the histogram indicates that the probability of the occurrence of each phase space value is uniform. Therefore, the predictability of a value is difficult. Hence, this signifies the presence of a strong chaos [25]. Hence, the histogram is a very simple visual tool to comprehend the dynamical behavior of any system.

Time Series Analysis

The time series analysis is a graphical inspection of the time series data, obtained by plotting the data series of the dynamic system versus time. It is a statistical analysis of the dynamic system, which represents the features of the data series. The features that are projected are periodicities and complexity of the data [37]. Here, time is considered as discrete, and labeled by the index i. The progress of the dynamical system is observed by pairing the time variable with the space variable, which is expressed as $(t_0, x_0), (t_1, f(x_0)), \ldots, (t_n, f^n(x_0)), \ldots$. The time series analysis is a straightforward method for complexity detection and can be used in both discrete and continuous dynamical systems.

Kaplan–Yorke Dimension or Lyapunov Dimension

The Kaplan–Yorke (KY) or Lyapunov dimension was defined as a conjecture relating the Lyapunov exponents and the Hausdorff (H) dimension of the dynamical system. The H-dimension of the attractor of a dissipative dynamical system is determined in terms of its Lyapunov exponents [45]. It quantifies the dimension of the chaotic attractor. A fraction dimension denotes that the attractor is a strange attractor.

Poincare Section

The Poincare map is essential in studying the flow of a system near a periodic orbit or a chaotic system. Consider S to be the surface of section in the system, where all the trajectories flow through it. Then, the Poincare map P is obtained by following the trajectories of the dynamical system, from one intersection of the trajectory with S to the next [46]. It is an effective method to study the motion features of the autonomous system, especially when observation of the characteristics of the flow is difficult using the phase portrait [47]. Poincare map helps in the identification of fixed points, periodic orbits and chaotic motion in a dynamical system. Hence, it is a potential tool to determine the characteristics of the flow in the system.

Correlation Dimension

Correlation dimension is a type of fractal dimension that portrays the space dimensionality of a series of points. It is a competent tool to measure the strangeness of an attractor of a dynamic system. The correlation dimension d is calculated with the following equation:

$$d = \lim_{r\to 0}\lim_{M\to\infty}\frac{\log C_e(r)}{\log r}, \quad (8)$$

where $\log C_e(r)$ is known as the correlation integral. A large value of correlation dimension denotes that the trajectories occupy space of a bigger dimensionality.

Further, the correlation dimension is used to exhibits the strangeness of the complex chaotic attractor [48, 49].

The key features of the chaos tests are summarized in Table 3.

The modified chaotic maps and systems are developed to have a better continuous and wider chaotic range. Analysis of the chaotic process with the tests briefed in Table 3 is a dire requirement before it is employed in different applications. This knowledge of the results of the chaos tests exhibiting the chaotic and non-chaotic behavior is essential for the key generation of the encryption algorithm.

Chaotic Maps and Systems Used in Image Encryption

This section is the heart of this review paper. Here, important properties of the dynamic system are presented and the chaos detection techniques used to analyze these systems are examined profoundly.

Survey of Discrete Chaotic Maps

Conventional chaotic maps such as logistic map, Arnold's cat map, tent map, sine map, and Henon are some of the commonly used maps for the confusion and diffusion process of image encryption. But due to their small and discontinuous chaotic range, they are modified to yield a better chaotic range than the original seed maps. New maps are designed by primarily introducing a nonlinear term, increasing the number of dimensions, control parameters or coupling seed maps. In this section, a comprehensive list of such conventional chaotic maps and modified chaotic maps are presented. Table 4 displays the list of chaotic maps and their important features.

The modified maps are analyzed with various chaos tests, to determine the nonlinear behavior and confirm the chaotic range. Table 5 highlights the tests used to investigate the modified maps listed in Table 4. The tick (✓) mark in Table 5 denotes the tests performed on the modified novel chaotic map. The other blank cells in the table denote that the corresponding tests were not performed on the modified map. The abbreviations of the tests titled in Tables 5, 6 and 7 are given as follows:

Bifurcation diagram—BD	Lyapunov exponent—LE
Phase portrait—PP	Sample entropy—SE
Kolmogorov–Sinai entropy—KE	Time series—TS
Three-state test—3ST	Histogram—Hist
Correlation dimension—CD	Permutation entropy—PE
Approximate entropy—AE	Poincare map—PCM
Lyapunov dimension—LD	

From Table 5, it is observed that the authors choose certain tests to analyze the maps developed. The bifurcation diagram and Lyapunov exponent are the most commonly used test to examine the behavior of the map.

Survey of Continuous Chaotic Systems

Rossler's system, Lorenz system, and Chen's system are popular chaotic systems used in image encryption. To improve the complex chaotic nature of the chaotic systems, some authors devise new systems with increased number of dimensions and with higher positive Lyapunov exponents. An inclusive number of modified and conventional chaotic systems are tabulated in Table 6.

The nonlinear nature of the chaotic system under different conditions of control parameter is analyzed with bifurcation diagram, Lyapunov exponent, phase portrait, time series analysis, Kaplan–Yorke or Lyapunov dimension and Poincare map. Table 7 lists the tests that are used to investigate the dynamic nature of the modified chaotic systems tabulated in Table 6. The tick (✓) mark denotes the tests performed to analyze the modified novel chaotic system. The blank cells in the table denote that the corresponding tests were not performed on the modified chaotic system.

Table 7 shows the various tests used to examine the chaotic systems. It is observed that phase portrait is widely used to analyze the chaotic attractor.

Discussion

In this section, the chaos detection techniques performed on the chaotic maps is discussed. Figures 4 and 5 compares the frequency of the tests used to examine the chaotic maps and systems based on the survey displayed in Tables 5 and 7, respectively.

It is observed from Fig. 4 that the bifurcation diagram and Lyapunov exponent are the most highly preferred chaos tests to analyze the nonlinear behavior of the chaotic maps. For 92% of the chaotic maps, the fixed points, periodic orbits and chaotic attractors are visualized, under different conditions of the control parameters with the bifurcation diagram. The chaotic range is determined with Lyapunov exponent for 88% of chaotic maps, and it is the second most frequently

Table 3 Chaos detection techniques with their importance

S. no	Chaos detection technique	Dynamical system	Importance	Observation
1.	Bifurcation diagram [50]	Chaotic map and system	It defines the qualitative change in the nature of a system, as a parameter is varied	1. Exhibits models of transitions 2. Identification of instabilities 3. Detect bifurcation points 4. Discover route to chaos
2. (a)	Lyapunov exponent (LE) [51]	Chaotic map	It measures the rate of separation or convergence with time, of initially two close trajectories	1. $(\lambda_1) = (-)$: fixed point for one-dimensional map 2. $(\lambda_1, \lambda_2) = (-, -)$: fixed point for two-dimensional map 3. $(\lambda_1, \lambda_2) = (0, -)$: limit cycle for two-dimensional map where λ denotes LE
2. (b)	Lyapunov exponent for chaotic system [51]	Chaotic system	1. Positive LE—chaotic 2. Negative LE—periodic 3. Zero LE—bifurcation point	1. $(\lambda_1, \lambda_2, \lambda_3) = (-, -, -)$: fixed point 2. $(\lambda_1, \lambda_2, \lambda_3) = (0, -, -)$: limit cycle 3. $(\lambda_1, \lambda_2, \lambda_3) = (0, 0, -)$: two-dimensional annulus 4. $(\lambda_1, \lambda_2, \lambda_3) = (+, +, -)$: instable limit cycle 5. $(\lambda_1, \lambda_2, \lambda_3) = (+, 0, 0)$: Instable two dimensions annulus 6. $(\lambda_1, \lambda_2, \lambda_3) = (+, 0, -)$: strange attractor
2. (c)	Lyapunov exponent (LE) for hyper-chaotic system [52]	4D hyper-chaotic system		1. 1 LE = 0, 3 LE < 0—periodic orbit 2. 2 LE = 0, 2 LE < 0—quasi-periodic orbit 3. 1 LE > 0, 1 LE = 0, 2 LE < 0—chaotic 4. 2 LE > 0—hyper-chaotic
3.	0–1 test [39, 53]	Chaotic map and system	It determines if a system is chaotic or non-chaotic	1. 0 K—non-chaotic 2. 1 K—chaotic
4.	Three-state test (3ST) [26, 54]	Chaotic map	It determines if a system is chaotic, quasi-periodic or periodic	1. $\lambda > 0$: chaotic 2. $\lambda < 0$: quasi-periodic 3. $\lambda = 0$: periodic
5.	Sample entropy [41, 42]	Chaotic map	It defines the measure for analyzing the chaos dynamics. It quantifies the complexity of the dynamic system	Larger sample entropy refers to lower level of regularity and therefore, it denotes the presence of higher complexity
6.	Kolmogorov entropy [55]	Chaotic map	It quantifies the amount of information required on an average to foretell the trajectory of the dynamical system in each unit time	1. Positive Kolmogorov entropy—unpredictable 2. Larger positive Kolmogorov entropy value—more unpredictability and better chaotic performance
7.	Phase portrait [56]	Chaotic map and system	It illustrates the topology of the system	Butterfly pattern—chaos in chaotic system
8.	Histogram [25]	Chaotic map and system	It exhibits the distribution of the phase values	1. Flat histogram: phase values are of equal probability 2. Curved histogram: phase values possess uneven distribution
9.	Time series analysis [28]	Chaotic map and system	It determines periodicity and chaos	1. Determines fixed points and limit cycles 2. Exhibits periodic oscillations 3. Illustrates erratic behavior

Table 3 (continued)

S. no	Chaos detection technique	Dynamical system	Importance	Observation
10.	Kaplan–Yorke dimension or Lyapunov dimension [45, 51]	Chaotic system	It measures the Lyapunov dimension, which is eigenvalue to describe chaos of system	It quantifies the dimension of the chaotic attractor. A non-integer dimension indicates that the attractor is a strange attractor
11.	Poincare section/first return map [46, 47, 57]	Chaotic map and system	It determines if the system is chaotic It exhibits the motion features of a multivariable autonomous system, which tells how the height of a trajectory changes after one lap around the cylinder It determines the stability of limit cycles	Masses of points concentrated in a certain areas depict chaotic region
12.	Correlation dimension [48]	Chaotic map	It tests the dimensionality of the occupied space of a series of points It tests the strangeness of the chaotic attractor	The larger the value of correlation dimension, the more chaotic the map is

used tests. The complexity of the chaotic maps is analyzed by only 32% of the chaotic maps with sample entropy.

The geometric representation of the trajectories of the chaotic maps is visualized in the phase plane with the phase portrait for only 28% of the chaotic maps. Further, only 16% of the chaotic maps measure the fractal dimension with correlation dimension and 12% of chaotic maps are analyzed statistically with time series analysis. Other chaos tests mentioned are used in meager, i.e., less than 10%. Among the 25 chaotic maps chosen for study, three-state test (3ST) was not considered by any of the authors for the analysis of the map.

The following conclusions have been analyzed and synthesized from Fig. 4 of the survey of the chaos detection techniques performed on the discrete chaotic maps

1. The geometric structure of the chaotic map is not wholly studied for most of the maps with the phase portrait diagram. Hence, the analysis of the chaotic dynamics of modified maps projects only partial result.
2. 0–1 test and 3ST owes the credit of analyzing the map in macro level [95]. Since 3ST is not performed for any of the maps, it strongly interprets that the nature of the dynamics (periodic, quasi-periodic, and chaotic) is not studied properly.
3. When a chaotic map is designed to secure and strengthen a cryptosystem, it is absolutely essential to know both the chaotic and non-chaotic range exhibited by that map [96]. Hence, this survey highlights the most crucial fact, that it is not just sufficient to identify the presence of the chaos with some chaos tests, but presenting the complete chaotic and non-chaotic range is extremely necessary. The consequence of the incomplete analysis of the chaotic map is stated in [94], where the author expresses the difficulty in choosing the input values for chaotic maps and systems and sometimes it is even highly complex and inaccurate. This may result in the cryptosystems to be weak and susceptible to attacks.

Next, the analysis of the chaos detection techniques used on the chaotic systems is performed in Fig. 5.

From Fig. 5, 100% of the authors certainly use the phase portrait to determine the geometric pattern of the chaotic systems. 66.77% of the chaotic systems are equally examined with the bifurcation diagram and time series analyses. This indicates that the dynamic behavior at various control parameters was examined and the aperiodicity was visualized for only 66.77% of the chaotic systems. The chaotic systems must possess at least one positive Lyapunov exponent. If it possesses more than one positive Lyapunov exponent, then the system is hyper-chaotic. This is examined only 61.11% of the time. 44.44% of the authors used the Poincare map to visualize the cross-section of the chaotic system and 27.78% used Kaplan dimension to

Table 4 List of chaotic maps and their corresponding number of dimensions, number of parameters and chaotic range

S. no	Chaotic maps	Mathematical equation	No of dimensions	No of control parameters	Chaotic range
1.	Logistic map [48, 58–60]	$f(x) = \lambda x(1-x)$	1	1	$r \in [3.54, 4]$
2.	Generalized logistic map [61, 62]	$f(x) = \frac{4\mu x(1-x)}{1+4(\mu^2-1)x(1-x)}$	1	1	$\mu \in [-0.6795, -0.4324]$
3.	Sine map [6, 42, 48]	$f(x) = \lambda \sin(\pi x)$	1	1	$\lambda \in [0.87, 1]$
4.	Squared sine logistic map [60]	$f(x) = rx(1-x) + \mu \sin^2(2\pi x)$	1	1	$r \in [3.5, 3.6]$
5.	Enhanced logistic map [48]	$x_{n+1} = \sin(\pi \tilde{a} x_n(1-x_n))$	1	1	$\tilde{a} \in (0, +\infty)$
6.	Enhanced sine map [48]	$x_{n+1} = \sin(\pi \tilde{\mu} \sin(\pi x_n))$	1	1	$\tilde{\mu} \in (0, +\infty)$
7.	Enhanced tent map [48]	$x_{n+1} = \begin{cases} \sin(\pi \tilde{r} x_i) & x_i < 0.5 \\ \sin(\pi \tilde{r}(1-x_i)) & x_i \geq 0.5 \end{cases}$	1	1	$\tilde{r} \in (0, +\infty)$
8.	Enhanced Henon map [48]	$\begin{cases} x_{i+1} = \sin(\pi(1-\tilde{a}x_i^2 + y_i)) \\ y_{i+1} = \sin(\pi \tilde{b} x_i) \end{cases}$	2	2	$\tilde{a} = 912$ $\tilde{b} = 39$
9.	Tent map [63]	$f(x,\mu) = \begin{cases} f_L(x,\mu) = \mu x, & x < 0.5 \\ f_R(x,\mu) = \mu(1-x), & \text{otherwise} \end{cases}$	1	1	$\mu \in [0, 2]$
10.	Modified logistic chaotic map [23]	$x_{n+1} = 2\beta - x_n^2/\beta$	1	1	Infinite key space, but cryptanalyzed in [22]
11.	Chebyshev map [64]	$z_{i+1} = \cos(w * \cos^{-1} z_i)$	1	1	$-1 \leq z_i \leq 1, w \in [2, 6]$ [2, 6]
12.	1D sine powered chaotic map (1DSP) [42]	$x_{n+1} = (x_n(\alpha+1))^{\sin(\beta\pi + x_n)}$	1	2	$\alpha \in [2.5, 4]$, $\beta \in [0.3, 0.4]$
13.	Logistic-sine–cosine (LSC) map [65]	$x_{n+1} = \cos(\pi(4rx_n(1-x_n) + (1-r)\sin(\pi x_n) - 0.5))$	1	1	$r \in [0, 1]$
14.	Sine-tent-cosine (STC) map [65]	$x_{n+1} = \begin{cases} \cos(\pi(r\sin(\pi x_n) + 2(1-r)x_n - 0.5)), & x_n < 0.5 \\ \cos(\pi(r\sin(\pi x_n) + 2(1-r)(1-x_n) - 0.5)), & x_n \geq 0.5 \end{cases}$	1	1	$r \in [0, 1]$
15.	Tent-logistic-cosine (TLC) map [65]	$x_{n+1} = \begin{cases} \cos(\pi(2rx_n + 4(1-r)x_n(1-x_n) - 0.5)), & x_n < 0.5 \\ \cos(\pi(2r(1-x_n) + 4(1-r)x_n(1-x_n) - 0.5)), & x_n \geq 0.5 \end{cases}$	1	1	$r \in [0, 1]$
16.	Logistic-tent system [24]	$x_{n+1} = \begin{cases} (rx_n(1-x_n) + (4-r)x_n/2) \bmod 1 & x_i < 0.5 \\ (rx_n(1-x_n) + (4-r)(1-x_n)/2) \bmod 1 & x_i \geq 0.5 \end{cases}$	1	1	$r \in (0, 1]$
17.	Logistic-sine system [24]	$x_{n+1} = (rx_n(1-x_n) + (4-r)\sin(\pi x_n)/4) \bmod 1$	1	1	$r \in (0, 1]$
18.	Tent-sine system [24]	$x_{n+1} = \begin{cases} (rx_n/2 + (4-r)\sin(\pi x_n)/4) \bmod 1 & x_i < 0.5 \\ (r(1-x_n)/2 + (4-r)\sin(\pi x_n)/4) \bmod 1 & x_i \geq 0.5 \end{cases}$	1	1	$r \in (0, 1]$
19.	Arnold's cat map [61, 61]	$\begin{pmatrix} x_{n+1} \\ y_{n+1} \end{pmatrix} = \begin{pmatrix} 1 & p \\ q & pq+1 \end{pmatrix} \begin{pmatrix} x_n \\ y_n \end{pmatrix} \bmod N$	2	2	$p, q \in \{0, 1, \ldots, N-1\}$
20.	Henon map [58, 58]	$x_{n+1} = 1 - ax_n^2 + y_n$ $y_{n+1} = bx_n$	2	2	$a = 1.4$ $b = 0.3$

Table 4 (continued)

S. no	Chaotic maps	Mathematical equation	No of dimensions	No of control parameters	Chaotic range
21.	2D logistic chaotic map [7]	$x_{n+1} = x_n u_1(1-x_n) + \lambda_1 y_n^2$ $y_{n+1} = y_n u_2(1-y_n) + \lambda_2(x_n^2 + x_n y_n)$	2	2	$2.75 < u_1 \leq 3.4$ $2.75 < u_2 \leq 3.45$ $0.15 < \lambda_1 \leq 0.21$ $0.13 < \lambda_2 \leq 0.15$
22.	Chaotic coupled sine map (CCSM) [67]	$x_{n+1} = \alpha\lvert\sin(\beta^3\pi x_n)\rvert + (1-\alpha)(1-\lvert\sin(\gamma^3\pi x_n(1-x_n))\rvert)$	1	3	$\alpha \in [0,1]$ $\beta, \gamma \in [8,10]$ [8, 10]
23.	2D Henon sine map [68]	$x_{n+1} = (1 - a\sin^2(x_n) + y_n) \bmod 1$ $y_{n+1} = bx_n \bmod 1$	2	2	$a \in (-\infty, -0.71] \cup [0.71, \infty)$ $b = 0.7$
24.	3D Chaotic cat map [11, 11]	$\begin{bmatrix} x_{n+1} \\ y_{n+1} \\ z_{n+1} \end{bmatrix} = A \begin{bmatrix} x_n \\ y_n \\ z_n \end{bmatrix} \bmod 1$	3	6	$a_x, b_x, a_y, b_y, a_z, b_z$ are positive numbers
25.	2DNLCML [30]	$x_{n+1}(i,j) = (1-\varepsilon)f[x_n(i,j)] + \frac{\varepsilon}{4}\{f[x_n(a,j)] + f[x_n(b,j)] + f[x_n(i,c)] + f[x_n(i,d)]\}$	1	6	$1 \leq i,j,a,b,c,d \leq L$ $0 \leq \varepsilon \leq 1$ $f(x) = \mu x(1-x), \mu \in (0,4]$
26.	Combinational chaotic system [25]	$x_{n+1} = \begin{cases} \omega_1 f_1 \circ F(r, x_n) + \alpha_1 g_1(rx_n) + \xi_1 \frac{(\beta_1 - r)x_n}{2} \bmod 1, & x_n < 0.5 \\ \omega_2 f_2 \circ F(r, x_n) + \alpha_2 g_2(rx_n) + \xi_2 \frac{(\beta_2 - r)x_n}{2} \bmod 1, & x_n \geq 0.5 \end{cases}$	1	9	$r \in (0,4]$
27.	2D-LICM hyper-chaotic map [70]	$x_{n+1} = \sin(21/(a(y_n+3)kx_n(1-kx_n)))$ $y_{n+1} = \sin(21/(a(kx_{n+1}+3)y_n(1-y_n)))$	2	2	$a \in (0.5, 1.969)$ $k \in (0.721, 1.4)$
28.	Beta chaotic map [71]	$x_{n+1} = k \times Beta(x_n; x_1, x_2, p, q),$ $p = b_1 + c_1 \times a$ $q = b_2 + c_2 \times a$	1	6	$a = [500 : 600]$
29.	Modified logistic map [72]	$z_{n+1} = \mu_z z_n(1-z_n)(1-z_n^2)$	1	1	$3.9 < \mu_z \leq 6.27$
30.	Higher-dimensional hyper-chaotic maps (HMC) [73]	$x_i(n+1) = K.F((f_i(x(n), b).$ $g(x_i(n), c)), a), \quad i = 1, 2, \ldots, m$	m-dimension	4	$k = 1, a = 2,$ $b = 4, c = \pi$ for 3 dimensional map 3D ICS-HMC
31.	Improved modified logistic map [74]	$x_{n+1} = [\mu x_n(1-x_n) \times 10^j] - \mu x_n(1-x_n) \times 10^j$	1	2	$0 \leq \mu \leq 4$ $2 \leq j \leq 8$
32.	4D chaotic map [75]	$x = p(ed)g$ $y = df$ $z = bde$ $w = d$	4	6	$p = 40, \quad b = 40,$ $d0 = 0 : 3, \quad e0 = 0 : 3,$ $f0 = 0 : 3, \quad g0 = 0 : 3$

measure the size of the attractor. It is observed that only 5.56% of the authors used the 0–1 test and complexity measure on the chaotic systems. The 0–1 test is a binary test, which does not require the phase space reconstruction, but directly determines chaos. But from the survey, it is clear that this test is seldom used.

The following analysis has been synthesized from the above survey of Fig. 5.

1. A comparison of Figs. 4 and 5 projects that chaotic systems are better analyzed, than its counterpart. Hence, a more complete investigation of the chaotic attractor, geometric shape, and equilibrium points is exhibited in chaotic systems, but not in chaotic maps.
2. Further, we bring the scope and limitations of the chaos identification measures to the limelight, which is discussed in [93]. It is pointed that though the phase por-

Table 5 Chaos detection techniques performed on the novel discrete chaotic maps tabulated in Table 4

S. no	Chaotic maps	Mathematical equation	BD	LE	PP	SE	KE	TS	0–1 test	3ST	Hist	CD	AE	PCM
1.	Generalized logistic map [62]	$f(x)=\frac{4\mu x(1-x)}{1+4(\mu^2-1)x(1-x)}$		✓										
2.	Squared sine logistic map [60]	$f(x)=rx(1-x)+\mu\sin^2(2\pi x)$	✓	✓										
3.	Enhanced logistic map [48]	$x_{n+1}=\sin(\pi\tilde{a}x_n(1-x_n)),\quad \tilde{a}\in(0,+\infty)$	✓	✓		✓						✓		
4.	Enhanced sine map [48]	$x_{n+1}=\sin(\pi\tilde{\mu}\sin(\pi x_n)),\quad \tilde{\mu}\in(0,+\infty)$	✓	✓		✓						✓		
5.	Enhanced tent map [48]	$x_{n+1}=\begin{cases}\sin(\pi\tilde{r}x_i) & x_i<0.5\\ \sin(\pi\tilde{r}(1-x_i)) & x_i\geq 0.5\end{cases}$	✓	✓		✓						✓		
6.	Enhanced Henon map [48]	$\begin{cases}x_{i+1}=\sin(\pi(1-\tilde{a}x_i^2+y_i))\\ y_{i+1}=\sin(\pi\tilde{b}x_i)\end{cases}$	✓	✓		✓						✓		
7.	Modified logistic chaotic map [23]	$x_{n+1}=2\beta-x_n^2/\beta$	✓	✓	✓									
8.	1D sine powered chaotic map (1DSP) [42]	$x_{n+1}=(x_n(\alpha+1))^{\sin(\beta\pi+x_n)}$	✓	✓	✓	✓		✓	✓					
9.	Logistic-sine–cosine (LSC) map [65]	$x_{n+1}=\cos(\pi(4rx_n(1-x_n)+(1-r)\sin(\pi x_n)-0.5))$	✓	✓		✓								
10.	Sine-tent-cosine (STC) map [65]	$x_{n+1}=\begin{cases}\cos(\pi(r\sin(\pi x_n)+2(1-r)x_n-0.5)), & x_n<0.5\\ \cos(\pi(r\sin(\pi x_n)+2(1-r)(1-x_n)-0.5)), & x_n\geq 0.5\end{cases}$	✓	✓		✓								
11.	Tent-logistic-cosine (TLC) map [65]	$x_{n+1}=\begin{cases}\cos(\pi(2rx_n+4(1-r)x_n(1-x_n)-0.5)), & x_n<0.5\\ \cos(\pi(2r(1-x_n)+4(1-r)x_n(1-x_n)-0.5)), & x_n\geq 0.5\end{cases}$	✓	✓		✓								
12.	Logistic-tent system [24]	$x_{n+1}=\begin{cases}(rx_n(1-x_n)+(4-r)x_n/2) \bmod 1 & x_i<0.5\\ (rx_n(1-x_n)+(4-r)(1-x_n)/2) \bmod 1 & x_i\geq 0.5\end{cases}$	✓	✓										
13.	Logistic-sine system [24]	$x_{n+1}=(rx_n(1-x_n)+(4-r)\sin(\pi x_n)/4) \bmod 1$	✓	✓										
14.	Tent-Sine system [24]	$x_{n+1}=\begin{cases}(rx_n/2+(4-r)\sin(\pi x_n)/4) \bmod 1 & x_i<0.5\\ (r(1-x_n)/2+(4-r)\sin(\pi x_n)/4) \bmod 1 & x_i\geq 0.5\end{cases}$	✓	✓										
15.	2D logistic chaotic map [7]	$x_{n+1}=x_nu_1(1-x_n)+\lambda_1y_n^2$ $y_{n+1}=y_nu_2(1-y_n)+\lambda_2(x_n^2+x_ny_n)$	✓											

Table 5 (continued)

S. no	Chaotic maps	Mathematical equation	BD	LE	PP	SE	KE	TS	0–1 test	3ST	Hist	CD	AE	PCM
16.	Chaotic coupled sine map (CCSM) [67]	$x_{n+1} = \alpha\lvert\sin(\beta^3\pi x_n)\rvert + (1-\alpha) \times (1 - \lvert\sin(\gamma^3\pi x_n(1-x_n))\rvert)$	✓	✓	✓									
17.	2D Henon Sine map [68]	$x_{n+1} = (1 - a\sin^2(x_n) + y_n) \bmod 1$ $y_{n+1} = bx_n \bmod 1$	✓	✓	✓									
18.	2DNLCML [30]	$x_{n+1}(i,j) = (1-\varepsilon)f[x_n(i,j)] + \frac{\varepsilon}{4}\{f[x_n(a,j)] + f[x_n(b,j)] + f[x_n(i,c)] + f[x_n(i,d)]\}$	✓				✓	✓						
19.	Combinational chaotic system [25]	$x_{n+1} = \begin{cases} \omega_1 f_1 \circ F(r,x_n) + \alpha_1 g_1(rx_n) + \xi_1 \frac{(\beta_1 - r)x_n}{2} \bmod 1, & x_n < 0.5 \\ \omega_2 f_2 \circ F(r,x_n) + \alpha_2 g_2(rx_n) + \xi_2 \frac{(\beta_2 - r)x_n}{2} \bmod 1, & x_n \geq 0.5 \end{cases}$	✓	✓				✓			✓			
20.	2D-LICM hyper-chaotic map [70]	$x_{n+1} = \sin(21/(a(y_n+3)kx_n(1-kx_n)))$ $y_{n+1} = \sin(21/(a(kx_{n+1}+3)y_n(1-y_n)))$	✓	✓	✓									
21.	Beta chaotic map [71]	$x_{n+1} = k \times Beta(x_n; x_1, x_2, p, q),$ $p = b_1 + c_1 \times a$ $q = b_2 + c_2 \times a$	✓											
22.	Modified logistic map [72]	$z_{n+1} = \mu_z z_n(1-z_n)(1-z_n^2)$	✓	✓									✓	
23.	Higher-dimensional hyper-chaotic maps (HMC) [73]	$x_i(n+1) = K.F((f_i(x(n), b)g(x_i(n), c)), a)$ $i = 1, 2, \ldots, m$	✓	✓	✓									
24.	Improved modified logistic map [74]	$x_{n+1} = \lceil \mu x_n(1-x_n) \times 10^j \rceil - \mu x_n(1-x_n) \times 10^j$	✓	✓										
25.	4D chaotic map [75]	$x = p(ed)g$ $y = df$ $z = bde$ $w = d$	✓	✓	✓									✓

Table 6 List of chaotic systems and their corresponding Lyapunov dimension, chaotic parameters and Lyapunov exponent

S. no	Chaotic system	Mathematical equation	LD	Chaotic parameter values	LE
1.	Lorenz system [76, 77]	$\dot{x} = -a(x-y)$ $\dot{y} = -xz + rx - y$ $\dot{z} = xy - bz$	2.062	$a = 10$ $r = 28$ $b = 8/3$	$\lambda_1 = 0.906$ $\lambda_2 = 0$ $\lambda_3 = -14.572$
2.	Lorenz hyper-chaotic system [77]	$\dot{x} = -a(x-y) + u$ $\dot{y} = -xz + rx - y$ $\dot{z} = xy - bz$ $\dot{u} = -xz + du$	3.05	$a = 10$ $r = 28$ $b = 8/3$ $d = 1.3$	$\lambda_1 = 0.39854$ $\lambda_2 = 0.24805$ $\lambda_3 = 0$ $\lambda_4 = -12.913$
3.	Rossler's system [28, 78]	$\dot{x} = -y - z$ $\dot{y} = x + ay$ $\dot{z} = b + z(x-c)$	2.005	$a = b = 0.2$ $c = 5.7$ [78]	$\lambda_1 = 0.072$ $\lambda_2 = 0$ $\lambda_3 = -13.79$
4.	Rossler's hyper-chaotic system [79]	$\dot{x} = -y - z$ $\dot{y} = x + ay + w$ $\dot{z} = b + xz$ $\dot{w} = -c + dw$	Not specified	$a = 0.25$ $b = 3$ $c = 0.5$ $d = 0.05$	Not specified
5.	Chua's circuit [28]	$\dot{x} = c_1(y - x - g(x))$ $\dot{y} = c_2(x - y + z)$ $\dot{z} = -c_3 y$ $g(x) = m_1 x + \frac{m_0 - m_1}{2}(\|x+1\| - \|x-1\|)$	Not specified	$c_1 = 15.6, c_2 = 1, c_3 = 25.58$ $m_o = -8/7, m_1 = -5/7$	Not specified
6.	Smooth hyper-chaotic Chua system [80]	$\dot{x}_1 = \alpha(x_2 - f(x_1))$ $\dot{x}_2 = x_1 - x_2 + x_3 + x_4$ $\dot{x}_3 = -\beta x_2 + x_4$ $\dot{x}_4 = -\gamma x_1 + \rho x_2 + \omega x_4$	Not specified	$\alpha = 9.5$ $\beta = 16$ $\gamma = 0.1$ $\rho = 0.6$ $\omega = 0.03$	$\lambda_1 > \lambda_2 > \lambda_3 > 0$ $\lambda_3 = 0$ $\lambda_1 + \lambda_2 + \lambda_4 < 0$
7.	Improper fractional-order laser chaotic system [81]	$D_t^q x_1 = \sigma(x_2 - x_1)$ $D_t^q x_2 = -x_2 - \delta x_3 + (\gamma - x_4)x_1$ $D_t^q x_3 = \delta x_2 - x_3$ $D_t^q x_4 = -bx_4 + x_1 x_2$	Not specified	$\sigma = 4, \quad \delta = 0.5$ $\gamma = 27, \quad b = 1.8$ $q = 1.005$	$\lambda_1 > 0, \lambda_2 > 0$ $\lambda_3 < 0, \lambda_4 < 0$
8.	5D HCCS [82, 82]	$\dot{x} = ay + cn$ $\dot{y} = -ax + bxw$ $\dot{z} = \mathrm{d}w$ $\dot{w} = -bxy - \mathrm{d}z$ $\dot{n} = -cx$	Not specified	$a = b = d = 30$ $c = 10, w = 1.850$ [82]	$\lambda_1 = 4.4$ $\lambda_2 = 0.12$ $\lambda_3 = 0$ $\lambda_4 = -0.12$ $\lambda_5 = -4.4$ [82]
9.	5D hyper-chaotic attractor [84]	$\dot{x}_1 = -ax_1 + x_2 x_3$ $\dot{x}_2 = -bx_2 + fx_5$ $\dot{x}_3 = -cx_3 + gx_4 + x_1 x_2$ $\dot{x}_4 = \mathrm{d}x_4 - hx_3$ $\dot{x}_5 = ex_5 - x_2 x_1^2$	3.624	$a = 10, \quad b = 60,$ $c = 20, \quad d = 15,$ $e = 40, \quad f = 1,$ $g = 50, \quad h = 10$ [85]	Not specified
10.	5D Hyper-chaotic system [47]	$\dot{x}_1 = a(x_2 - x_1) + x_2 x_3 x_4$ $\dot{x}_2 = b(x_1 + x_2) + x_5 - x_1 x_3 x_4$ $\dot{x}_3 = -cx_2 - \mathrm{d}x_3 - ex_4 + x_1 x_2 x_4$ $\dot{x}_4 = -fx_4 + x_1 x_2 x_3$ $\dot{x}_5 = -g(x_1 + x_2)$	Not specified	$a = 30, \quad b = 10,$ $c = 15.7, \quad d = 5,$ $e = 2.5, \quad f = 4.45,$ $g = 38.5$	$\lambda_1 = 5.12$ $\lambda_2 = 0.90$ $\lambda_3 = 0$ $\lambda_4 = -10.41$ $\lambda_5 = -25.08$
11.	A new chaotic attractor [86]	$\dot{x} = a(y-x)$ $\dot{y} = -xz + cy$ $\dot{z} = xy - bz$	Not specified	$a = 36$ $b = 3$ $c = 20$	$\lambda_1 = 1.5046$ $\lambda_2 = 0$ $\lambda_3 = -22.5044$ [87]

Table 6 (continued)

S. no	Chaotic system	Mathematical equation	LD	Chaotic parameter values	LE
12.	Chen's hyper-chaotic system [88]	$\dot{x}_1 = a(x_2 - x_1)$ $\dot{x}_2 = -x_1x_3 + dx_1 + cx_2 - x_4$ $\dot{x}_3 = x_1x_2 - bx_3$ $\dot{x}_4 = x_4 + k$	Not specified	$a = 36,\ b = 3,$ $c = 28,\ d = -16,$ $k = 0.2$	$\lambda_1 = 1.552$ $\lambda_2 = 0.023$ $\lambda_3 = 0$ $\lambda_4 = -12.573$
13.	Liu chaotic system [52, 89]	$\dot{x} = a(y - x)$ $\dot{y} = bx - kxz$ $\dot{z} = -cz + hx^2$	Not specified	$a = 10,\ b = 40,$ $c = 2.5,\ k = 1,$ $h = 4$	$\lambda_1 = 1.64328$ $\lambda_2 = 0$ $\lambda_3 = -14.42$
14.	Liu hyper-chaotic system [52]	$\dot{x} = a(y - x)$ $\dot{y} = bx - kxz + w$ $\dot{z} = -cz + hx^2$ $\dot{w} = -dx$	3.0927	$a = 10,\ b = 40,$ $c = 2.5,\ k = 1,$ $h = 4,\ d = 10.6$	$\lambda_1 = 1.1491$ $\lambda_2 = 0.12688$ $\lambda_3 = 0$ $\lambda_4 = -13.767$
15.	5D hyper-chaotic Lorenz system [90]	$\dot{x}_1 = a(x_2 - x_1) + x_4 + x_5$ $\dot{x}_2 = cx_1 - x_1x_3 - x_2$ $\dot{x}_3 = x_1x_2 - bx_3$ $\dot{x}_4 = -x_1x_3 + px_4$ $\dot{x}_5 = qx_1$	4.0159	$a = 10$ $b = 8/3$ $c = 28$ $p = 1.3$ $q = 2.5$	$\lambda_1 = 0.4195$ $\lambda_2 = 0.2430$ $\lambda_3 = 0.0145$ $\lambda_4 = 0$ $\lambda_5 = -13.0405$
16.	Reversals of the Earth's geomagnetic field [50]	$\dot{Q} = \mu Q - VD$ $\dot{D} = -\nu D + VQ$ $\dot{V} = \Gamma - V + QD$	Not specified	$\mu = 0.3$ $\nu = 0.2$ $\Gamma = 5$	$\lambda = 0.1$(only 1 LE is specified)
17.	Novel chaotic system (NCS) [56]	$\dot{x} = ax - yz$ $\dot{y} = -by + xz$ $\dot{z} = c - z + xy + dzy$	2.194	$a = 0.7$ $b = 0.1$ $c = 0.001$ $d = 0.1$	$\lambda_1 = 0.1211$ $\lambda_2 = 0$ $\lambda_3 = -0.625$
18.	Memristive hyper-chaotic system [91]	$\dot{x} = a[W(w)(y - x) - h(x)]$ $\dot{y} = W(w)(x - y) + z$ $\dot{z} = -by - cz$ $\dot{w} = y - x$	Not specified	$a = 30,\ b = 36,$ $d = 2.5,\ e = 3.5,$ $m_0 = -0.5,\ m_1 = -0.1$ $c \in [0.073, 0.162]$	$\lambda_1 = 0.317$ $\lambda_2 = 0.063$ $\lambda_3 = 0.001$ $\lambda_4 = -11.90$
19.	4D dynamic system [92]	$\dot{x} = -ax - e\omega + yz$ $\dot{y} = by + xz$ $\dot{z} = cz + f\omega - xy$ $\dot{\omega} = d\omega - gz$	Not specified	$a = 50,\ b = -16,$ $c = 10,\ d = 0.2,$ $e = 10,\ f = 16,$ $g = 0.5$	$\lambda_1 = 2.4736$ $\lambda_2 = 0.5175$ $\lambda_3 = 0$ $\lambda_4 = -58.7248$
20.	Seven-dimensional fractional-order chaotic system [93]	$\frac{d^\alpha x}{dt^\alpha} = a(y - x) + w - u - v$ $\frac{d^\beta y}{dt^\beta} = cx - y - xz - p$ $\frac{d^\delta z}{dt^\delta} = -bz + xy$ $\frac{d^\epsilon w}{dt^\epsilon} = nw - yz$ $\frac{d^\gamma u}{dt^\gamma} = ev + yz$ $\frac{d^\lambda v}{dt^\lambda} = rx$ $\frac{d^\eta p}{dt^\eta} = fx + yz$	Not specified	$a = 10,\ b = 8/3,\ c = 28,$ $n = -1,\ e = 8,\ f = 1,\ r = 5,$ $\alpha = \beta = \delta = \varepsilon = \gamma = \lambda = \eta = 0.9$	Not specified

trait is simple, the accuracy is not satisfactory. Further, the Poincare map fails to differentiate chaos and random motion. In addition, the calculation of the largest Lyapunov exponent is not direct. Since, each chaos detection technique has a particular limitation, using few tests will project partial dynamics of the novel system.

Table 7 Chaos detection techniques performed on novel continuous chaotic systems tabulated in Table 6

S. no	Chaotic system	Mathematical equation	BD	LE	PP	TS	LD	PCM	0–1 test	SE
1.	Lorenz hyper-chaotic system [77]	$\dot{x} = -a(x - y) + u$ $\dot{y} = -xz + rx - y$ $\dot{z} = xy - bz$ $\dot{u} = -xz + \mathrm{d}u$	✓	✓	✓	✓	✓	✓		
2.	Rossler's hyper-chaotic system [79]	$\dot{x} = -y - z$ $\dot{y} = x + ay + w$ $\dot{z} = b + xz$ $\dot{w} = -c + \mathrm{d}w$			✓			✓		
3.	Chua's circuit [28]	$\dot{x} = c_1(y - x - g(x))$ $\dot{y} = c_2(x - y + z)$ $\dot{z} = -c_3 y$ $g(x) = m_1 x + \frac{m_0 - m_1}{2}$ $(\lvert x + 1\rvert - \lvert x - 1\rvert)$			✓					
4.	Smooth hyper-chaotic Chua system [80]	$\dot{x}_1 = \alpha(x_2 - f(x_1))$ $\dot{x}_2 = x_1 - x_2 + x_3 + x_4$ $\dot{x}_3 = -\beta x_2 + x_4$ $\dot{x}_4 = -\gamma x_1 + \rho x_2 + \omega x_4$	✓	✓	✓		✓			
5.	Improper fractional-order laser chaotic system [81]	$D_t^q x_1 = \sigma(x_2 - x_1)$ $D_t^q x_2 = -x_2 - \delta x_3 + (\gamma - x_4)x_1$ $D_t^q x_3 = \delta x_2 - x_3$ $D_t^q x_4 = -bx_4 + x_1 x_2$	✓	✓	✓	✓				
6.	5D HCCS [82, 82]	$\dot{x} = ay + cn$ $\dot{y} = -ax + bxw$ $\dot{z} = \mathrm{d}w$ $\dot{w} = -bxy - \mathrm{d}z$ $\dot{n} = -cx$	✓	✓	✓	✓		✓		
7.	5D hyper-chaotic attractor [84]	$\dot{x}_1 = -ax_1 + x_2 x_3$ $\dot{x}_2 = -bx_2 + fx_5$ $\dot{x}_3 = -cx_3 + gx_4 + x_1 x_2$ $\dot{x}_4 = \mathrm{d}x_4 - hx_3$ $\dot{x}_5 = ex_5 - x_2 x_1^2$	✓	✓	✓	✓	✓	✓		

Table 7 (continued)

S. no	Chaotic system	Mathematical equation	BD	LE	PP	TS	LD	PCM	0–1 test	SE
8.	5D hyper-chaotic system [47]	$\dot{x}_1 = a(x_2 - x_1) + x_2x_3x_4$ $\dot{x}_2 = b(x_1 + x_2) + x_5 - x_1x_3x_4$ $\dot{x}_3 = -cx_2 - \mathrm{d}x_3 - ex_4 + x_1x_2x_4$ $\dot{x}_4 = -fx_4 + x_1x_2x_3$ $\dot{x}_5 = -g(x_1 + x_2)$	✓	✓	✓	✓		✓		
9.	A new chaotic attractor [86]	$\dot{x} = a(y - x)$ $\dot{y} = -xz + cy$ $\dot{z} = xy - bz$			✓					
10.	Chen's hyper-chaotic system [88]	$\dot{x}_1 = a(x_2 - x_1)$ $\dot{x}_2 = -x_1x_3 + \mathrm{d}x_1 + cx_2 - x_4$ $\dot{x}_3 = x_1x_2 - bx_3$ $\dot{x}_4 = x_4 + k$			✓					
11.	Liu chaotic system [89, 89]	$\dot{x} = a(y - x)$ $\dot{y} = bx - kxz$ $\dot{z} = -cz + hx^2$	✓		✓	✓		✓		
12.	Liu hyper-chaotic system [52]	$\dot{x} = a(y - x)$ $\dot{y} = bx - kxz + w$ $\dot{z} = -cz + hx^2$ $\dot{w} = -\mathrm{d}x$	✓	✓	✓	✓				
13.	5D hyper-chaotic Lorenz system [90]	$\dot{x}_1 = a(x_2 - x_1) + x_4 + x_5$ $\dot{x}_2 = cx_1 - x_1x_3 - x_2$ $\dot{x}_3 = x_1x_2 - bx_3$ $\dot{x}_4 = -x_1x_3 + px_4$ $\dot{x}_5 = qx_1$		✓	✓	✓	✓			
14.	Reversals of the Earth's geomagnetic field [50]	$\dot{Q} = \mu Q - VD$ $\dot{D} = -vD + VQ$ $\dot{V} = \Gamma - V + QD$	✓	✓	✓	✓		✓		
15.	Novel chaotic system (NCS) [56]	$\dot{x} = ax - yz$ $\dot{y} = -by + xz$ $\dot{z} = c - z + xy + \mathrm{d}zy$	✓	✓	✓	✓	✓			

Table 7 (continued)

S. no	Chaotic system	Mathematical equation	BD	LE	PP	TS	LD	PCM	0–1 test	SE
16.	Memristive hyper-chaotic system [91]	$\dot{x} = a[W(w)(y - x) - h(x)]$ $\dot{y} = W(w)(x - y) + z$ $\dot{z} = -by - cz$ $\dot{w} = y - x$			✓	✓				
17.	4D dynamic system [92]	$\dot{x} = -ax - e\omega + yz$ $\dot{y} = by + xz$ $\dot{z} = cz + f\omega - xy$ $\dot{\omega} = \mathrm{d}\omega - gz$	✓	✓	✓	✓		✓		
18.	Seven-dimensional fractional-order chaotic.system [93]	$\frac{\mathrm{d}^{\alpha}x}{\mathrm{d}t^{\alpha}} = a(y - x) + w - u - v$ $\frac{\mathrm{d}^{\beta}y}{\mathrm{d}t^{\beta}} = cx - y - xz - p$ $\frac{\mathrm{d}^{\delta}z}{\mathrm{d}t^{\delta}} = -bz + xy$ $\frac{\mathrm{d}^{\epsilon}w}{\mathrm{d}t^{\epsilon}} = nw - yz$ $\frac{\mathrm{d}^{\gamma}u}{\mathrm{d}t^{\gamma}} = ev + yz$ $\frac{\mathrm{d}^{\lambda}v}{\mathrm{d}t^{\lambda}} = rx$ $\frac{\mathrm{d}^{\eta}p}{\mathrm{d}t^{\eta}} = fx + yz$	✓		✓				✓	✓

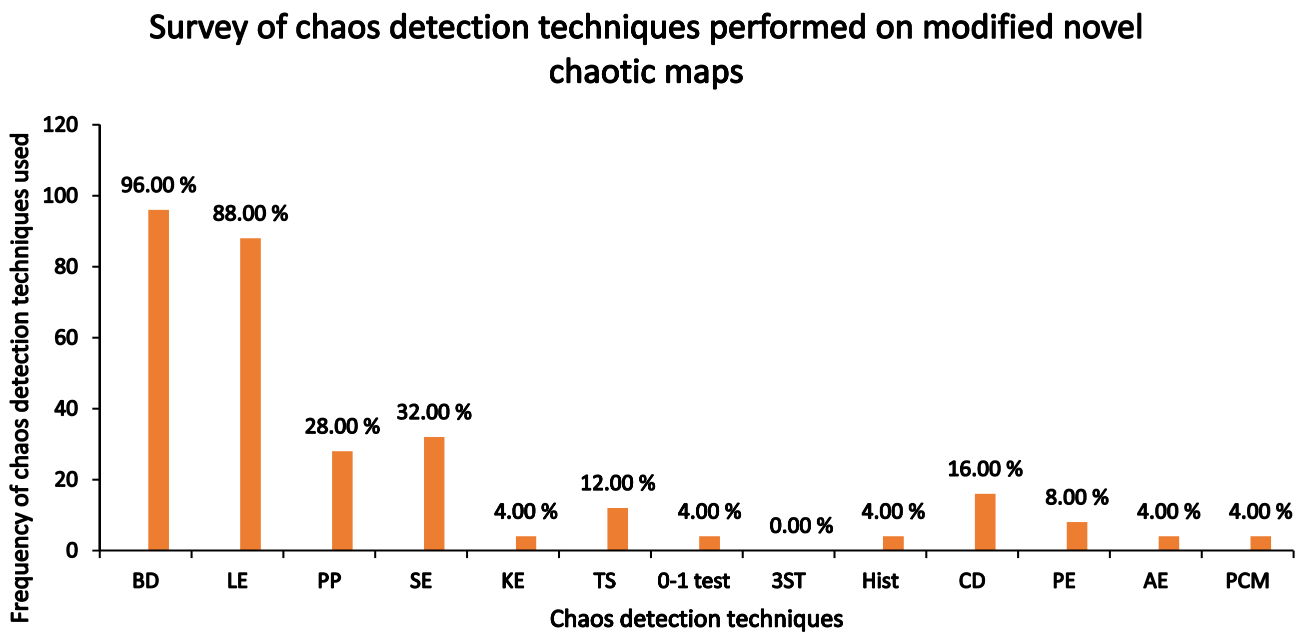

Fig. 4 Survey of chaos detection techniques performed on novel discrete chaotic maps

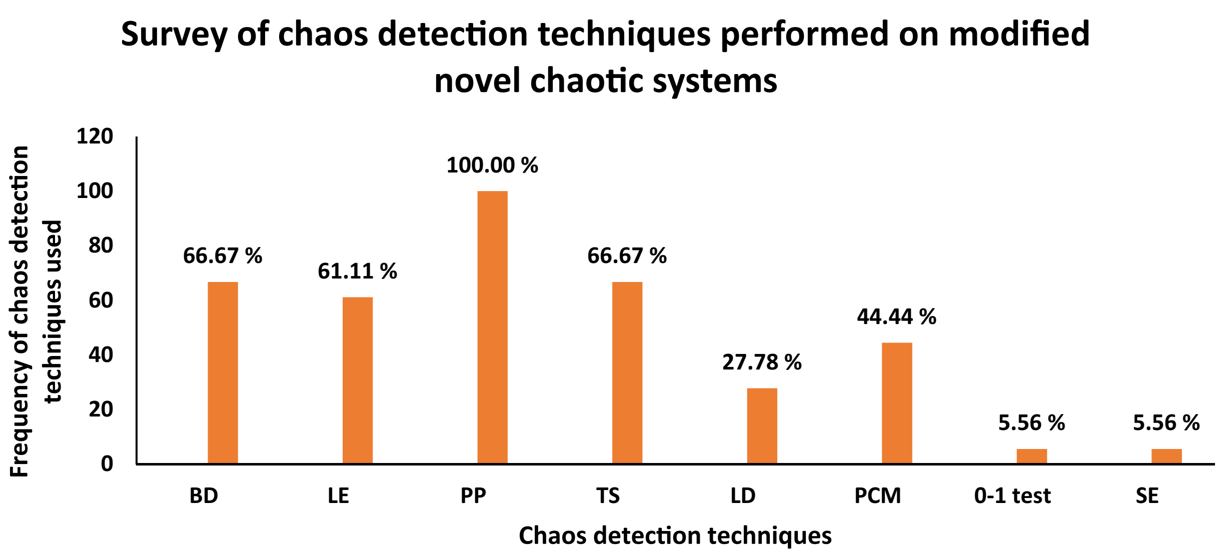

Fig. 5 Survey of chaos detection techniques performed on novel continuous chaotic systems

3. The analysis paramount that each chaos detection techniques have its own pros and cons. The tests projects a particular aspect of the nature of the dynamical system. Hence, this review paper emphasizes the importance of performing various tests on chaotic maps and systems for understanding the complete dynamics of the novel system.

By overcoming all these issues, the chaotic systems can be used to its full potential in various applications [96]–[99].

Conclusion

In this paper, a review of chaos detection techniques performed on 25 discrete chaotic maps and 18 continuous chaotic systems brought to the fore that a complete analysis of the some modified chaotic maps and chaotic systems has not been provided. Emphasis is made that it is essential to understand the importance and limitations of each test. Observation from the survey shows that chaotic systems are examined better than the chaotic maps. Further, the bifurcation diagram and Lyapunov exponent are the most preferred test to analyze the chaotic map and phase portrait diagram for the chaotic system. Though these tests reveal some significant results, they do not provide a comprehensive understanding of the complete behavior of the chaotic process. Other tests such as 0–1 test, three-state test and some entropy tests are given meager importance. The incomplete analysis of a novel dynamic system may lead to insufficient and undiscovered knowledge of the parameters and conditions of the chaotic process. Such maps and systems prove to be theoretically strong, but they do not cater the practical and real time needs of security issues. This will impact the development of a chaos-based image cryptosystem. It is also not a necessary condition to perform all the tests on the chaotic process, but it is essential to choose the appropriate chaos detection technique and provide a complete analysis of the chaotic process. Therefore, it is strongly emphasized and recommended that a more profound experiment and analysis be performed on the novel chaotic maps and systems, for building a secure chaos-based image cryptosystem that is resistant to different attacks.

Funding The authors did not receive support from any organization for the submitted work.

Code Availability Not applicable.

Declarations

Conflict of Interest The authors have no conflict of interest to declare that are relevant to the content of this article.

Availability of Data and Material and Code Not applicable.

References

1. Wang X, Wang S, Zhang Y, Luo C. A one-time pad color image cryptosystem based on SHA-3 and multiple chaotic systems. Opt Lasers Eng. 2018;103:1–8.
2. Radwan AG, AbdElHaleem SH, Abd-El-Hafiz SK. Symmetric encryption algorithms using chaotic and non-chaotic generators : A review. J Adv Res. 2016;7(2):193–208.
3. Murugan CA, Karthigaikumar P. Survey on image encryption schemes, bio cryptography and efficient encryption algorithms. Mob Netw Appl. 2018;1–6. https://doi.org/10.1007/s11036-018-1058-3.
4. Li C, Zhang Y, Yong E. When an attacker meets a cipher-image in 2018: a year in review. J Inf Secur Appl. 2019;48:2361.
5. Movafegh H, Nodehi A, Enayatifar R. An overview of encryption algorithms in color images. Signal Process. 2019;164:163–85.
6. Kalpana J, Murali P. An improved color image encryption based on multiple DNA sequence operations with DNA synthetic image and chaos. Optik. 2015;126(24):5703–9.
7. Chai X, Chen Y, Broyde L. A novel chaos-based image encryption algorithm using DNA sequence operations. Opt Lasers Eng. 2017;88:197–213.
8. Zarebnia M, Kianfar R, Parvaz R. Multi-color image compression-encryption algorithm based on chaotic system and fuzzy transform. Multimed Tools Appl. 2019;78:10491–511.
9. Vidhya R, Brindha M. A novel conditional Butterfly Network Topology based chaotic image encryption. J Inf Secur Appl. 2020;52:102484.
10. Maddodi G, Awad A, Awad D, et al. A new image encryption algorithm based on heterogeneous chaotic neural network generator and DNA encoding. Multimed Tools Appl. 2018;77:24701–25.
11. Niyat AY, Moattar MH, Torshiz MN. Color image encryption based on hybrid hyper-chaotic system and cellular automata. Opt Lasers Eng. 2017;90(90):225–37.
12. Sayed WS, Ismail SM, Said LA, Radwan AG. On the fractional order generalized discrete maps. In: Azar AT, Radwan AG, Vaidyanathan S, editors. Mathematical Techniques of Fractional Order Systems. Elsevier Inc.; 2018. https://doi.org/10.1016/B978-0-12-813592-1.00013-1.
13. Hosny KM. Multimedia security using chaotic maps: principles and methodologies. New York: Springer; 2020.
14. Özkaynak F. Brief review on application of nonlinear dynamics in image encryption. Nonlinear Dyn. 2018;92(2):305–13.
15. Tanwar G, Mishra N. Survey on image encryption techniques. Int J Adv Res Comput Sci Softw Eng. 2015;5(12):563–9.
16. Jain Y, Bansal R, Sharma G, et al. Image encryption schemes : A complete survey. Int J Signal Process Image Process Pattern Recognit. 2016;9(7):157–92.
17. Younes MAB. Literature survey on different techniques of image encryption. Int J Sci Eng Res. 2016;7(1):93–8.
18. Kumar HSR, Safeeriya SPF, Aithal G, Shetty S. A survey on key(s) and keyless image encryption techniques. Cybern Inf Technol. 2017;17(4):134–64.
19. Sharma M, Kowar MK. Image encryption techniques using chaotic schemes: a review. Int J Eng Sci Technol. 2010;2(6):2359–63.
20. Srivastava A. A survey report on different techniques of image encryption. Int J Emerg Technol Adv Eng. 2012;2:163–7.
21. Suneja K, Dua S, Dua M. A review of chaos based image encryption. In: Proc. 3rd Int. Conf. Comput. Methodol. Commun. ICCMC 2019; 2019. pp. 693–8.
22. Muthu JS, Murali P. Comment on "An image encryption algorithm based on modified logistic chaotic map." Opt Int J Light Electron Opt. 2019;207:163843.
23. Han C. An image encryption algorithm based on modified logistic chaotic map. Opt Int J Light Electron Opt. 2019;181:779–85.
24. Zhou Y, Bao L, Chen CLP. A new 1D chaotic system for image encryption. Signal Process. 2014;97:172–82.
25. Parvaz R, Zarebnia M. A combination chaotic system and application in color image encryption. Opt Laser Technol. 2018;101:30–41.
26. Eyebe Fouda JSA, Effa JY, Kom M, Ali M. The three-state test for chaos detection in discrete maps. Appl Soft Comput J. 2013;13(12):4731–7.
27. Davidovits P. Physics in biology and medicine, 5th edn. Elsevier; 2019. https://doi.org/10.1016/B978-0-12-813716-1.00010-0.
28. Alligood KT, Sauer TD, Yorke JA. CHAOS : An introduction to dynamical systems. New York: Springer; 1996.
29. Szemplinska-Stupnicka W. Chaos, bifurcations and fractals around us. World Sci Ser Nonlinear Sci; 2003. https://doi.org/10.1142/5419.
30. Zhang Y, He Y, Li P, Wang X. A new color image encryption scheme based on 2DNLCML system and genetic operations. Opt Lasers Eng. 2020;128:106040.

31. Zhang Y-Q, Wang X-Y. A symmetric image encryption algorithm based on mixed linear–nonlinear coupled map lattice. Inf Sci (N Y). 2014;273:329–51.
32. Gayathri J, Subashini S. A survey on security and efficiency issues in chaotic image encryption. Int J Inf Comput Secur. 2016;8:347–81.
33. Suri S, Vijay R. A Pareto-optimal evolutionary approach of image encryption using coupled map lattice and DNA. Neural Comput Appl. 2019. https://doi.org/10.1007/s00521-019-04668-x.
34. Arumugham S, Rajagopalan S, Rethinam S, et al. Synthetic image and strange attractor: two folded encryption approach for secure image communication. Adv Intell Syst Comput. 2020;1082:467–78.
35. Xue H, Du J, Li S, Ma W. Region of interest encryption for color images based on a hyperchaotic system with three positive Lyapunov exponents. Opt Laser Technol. 2018;106:506–16.
36. Çavuşoğlu Ü, Panahi S, Akgül A, et al. A new chaotic system with hidden attractor and its engineering applications: analog circuit realization and image encryption. Analog Integr Circuits Signal Process. 2019;98(1):85–99.
37. Rüdisüli M, Schildhauer TJ, Biollaz SMA, Van Ommen JR. Fluidized bed technologies for near-zero emission combustion and gasification; 2013. https://doi.org/10.1533/9780857098801.3.813.
38. Sun KH, Liu X, Zhu CX. The 0–1 test algorithm for chaos and its applications. Chin Phys B. 2010;19(11):7.
39. Gottwald GA, Melbourne I. The 0–1 test for chaos: a review. Lect Notes Phys. 2016;915:221–47.
40. Delgado-Bonal A, Marshak A. Approximate entropy and sample entropy: A comprehensive tutorial. MDPI. 2019. https://doi.org/10.3390/e21060541.
41. Li N, Pan W,Xiang S, , et al. Quantifying the complexity of the chaotic intensity of an external-cavity semiconductor laser via sample entropy. IEEE J Quantum Electron. 2014. https://doi.org/10.1109/JQE.2014.2344691.
42. Mansouri A, Wang X. A novel one-dimensional sine powered chaotic map and its application in a new image encryption scheme. Inf Sci (N Y). 2020. https://doi.org/10.1016/j.ins.2020.02.008.
43. Xiong H, Shang P, He J, Zhang Y. Complexity and information measures in planar characterization of chaos and noise. Nonlinear Dyn. 2020;100(2):1673–87.
44. Tucker W. Studies in computational intelligence. Berlin, Heidelberg: Springer; 2008.
45. Evans DJ, Cohen EGD, Searles DJ, Bonetto F. Note on the Kaplan-Yorke dimension and linear transport coefficients. J Stat Phys. 2000;101(1–2):17–34.
46. Strogatz SH. NonLinear dynamics and chaos. New York: Perseus Books Publishing; 1994.
47. Fan B, Tang LR. A new five-dimensional hyperchaotic system and its application in DS-CDMA. In: Proceedings - 2012 9th International Conference on Fuzzy Systems and Knowledge Discovery (FSKD 2012); 2012. pp. 2069–73.
48. Hua Z, Zhou B, Zhou Y. Sine chaotification model for enhancing chaos and its hardware implementation. IEEE Trans Ind Electron. 2019;66(2):1273–84.
49. Hua Z, Yi S, Zhou Y, et al. Designing hyperchaotic cat maps with any desired number of positive lyapunov exponents. IEEE Trans Cybern. 2018;48(2):463–73.
50. Gissinger C. A new deterministic model for chaotic reversals. Eur Phys J B. 2012. https://doi.org/10.1140/epjb/e2012-20799-5.
51. Shi W. Lyapunov exponent analysis to chaotic phenomena of marine power system. IFAC Fault Detect Superv Saf Tech Process.. 2007;2:1497–502.
52. Fa-Qiang W, Chong-Xin L. Hyperchaos evolved from the Liu chaotic system. Chin Phys. 2006;15(5):0963–1006.
53. Gottwald GA, Melbourne I, A PRSL. A new test for chaos in deterministic systems. Proceedings R Soc. 2004:603–11. https://doi.org/10.1098/rspa.2003.1183.
54. Eyebe Fouda JSA, Koepf W. Efficient detection of the quasi-periodic route to chaos in discrete maps by the three-state test. Nonlinear Dyn. 2014;78(2):1477–87.
55. Zhou Y, Hua Z, Pun C, Chen CLP. Cascade chaotic system with applications. IEEE Trans Cybern. 2015;45(9):1–12.
56. Rajagopal K, Akgul A, Moroz IM, et al. A simple chaotic system with topologically different attractors. IEEE Access. 2019;7:89936–47.
57. Bouslehi H, Seddik H. A new rapid hyperchaotic system for more efficient 2D data encryption. Multimed Tools Appl. 2018;77(6):7741–62.
58. Dellnitz M, Junge O. Handbook of dynamical systems. Amsterdam: Elsevier B.V; 2002.
59. Pareek NK, Patidar V, Sud KK. Image encryption using chaotic logistic map. Image Vis Comput. 2006;24(9):926–34.
60. de Carvalho RE, Leonel ED. Squared sine logistic map. Phys A Stat Mech Appl. 2016;463:37–44.
61. Krishnamoorthi R, Murali P. A selective image encryption based on square-wave shuffling with orthogonal polynomials transformation suitable for mobile devices. Multimed Tools Appl. 2017;76(1):1217–46.
62. Bhatnagar G, Wu QMJ. Selective image encryption based on pixels of interest and singular value decomposition. Digit Signal Process. 2012;1:1–16.
63. Li C, Luo G, Qin K. An image encryption scheme based on chaotic tent map. Nonlinear Dyn. 2017;87(1):127–33.
64. Liu H, Wang X. Image encryption using DNA complementary rule and chaotic maps. Appl Soft Comput J. 2012;12(5):1457–66.
65. Hua Z, Zhou Y, Huang H. Cosine-transform-based chaotic system for image encryption. Inf Sci (NY). 2019;480:403–19.
66. Chen F, Wong K, Liao X, Xiang T. Period distribution of generalized discrete Arnold cat map. Theor Comput Sci. 2014;552:13–25.
67. Yosefnezhad B, Peyman I, Jabalkandi FA, et al. Digital image scrambling based on a new one-dimensional coupled Sine map Behzad. Nonlinear Dyn. 2019;97:2693–721.
68. Wu J, Liao X, Yang B. Image encryption using 2D Henon—Sine map and DNA approach. Signal Process. 2018. https://doi.org/10.1016/j.sigpro.2018.06.008.
69. Chen G, Mao Y, Chui CK. A symmetric image encryption scheme based on 3D chaotic cat maps. 2004;21:749–61.
70. Cao C, Sun K, Liu W. A novel bit-level image encryption algorithm based on 2D-LICM hyperchaotic map. Signal Process. 2017. https://doi.org/10.1016/j.sigpro.2017.08.020.
71. Zahmoul R, Ejbali R, Zaied M. Image encryption based on new Beta chaotic maps. Opt Lasers Eng. 2017;96(April):39–49.
72. Hanis S, Amutha R. A fast double-keyed authenticated image encryption scheme using an improved chaotic map and a butterfly-like structure. Nonlinear Dyn. 2018;95:421–32.
73. Chen C, Sun K, He S. A class of higher-dimensional hyperchaotic maps. Eur Phys J Plus. 2019. https://doi.org/10.1140/epjp/i2019-12776-9.
74. Attaullah, Shah T, Jamal SS. An improved chaotic cryptosystem for image encryption and digital watermarking. Wirel Pers Commun. 2020;110(3):1429–42.
75. Gupta A, Singh D, Kaur M. An efficient image encryption using non-dominated sorting genetic algorithm—III based 4—D chaotic maps. J Ambient Intell Humaniz Comput. 2019. https://doi.org/10.1007/s12652-019-01493-x.
76. Kudryashov NA. Analytical Solutions of the Lorenz System. Regul Chaotic Dyn. 2015;20(2):123–33.
77. Jia Q. Hyperchaos generated from the Lorenz chaotic system and its control. Phys Lett A. 2007;366:217–22.

78. Rossler OE. An equation for continuous chaos. Phys Lett. 1976;57A(5):397–8. https://doi.org/10.1016/0375-9601(76)90101-8.
79. Rossler OE. An equation for hyperchaos. Phys Lett. 1979;71A(23):155–7.
80. Xi H, Yu S, Zhang Z, Deng K. Generation of hyperchaotic Chua system via state feedback control. In: 2010 International Workshop on Chaos-fractals Theories and Applications. IEEE; 2010. https://doi.org/10.1109/IWCFTA.2010.45.
81. Yang F, Mou J, Ma C, Cao Y. Dynamic analysis of an improper fractional-order laser chaotic system and its image encryption application. Opt Lasers Eng. 2020;129:106031.
82. Dong E, Yuan M, Du S, Chen Z. A new class of Hamiltonian conservative chaotic systems with multistability and design of pseudo-random number generator. Appl Math Model. 2019;73:40–71.
83. Zhou M, Wang C. A novel image encryption scheme based on conservative hyperchaotic system and closed-loop diffusion between blocks. Signal Process. 2020;171:107484.
84. Zarei A. Complex dynamics in a 5-D hyper-chaotic attractor with four-wing, one equilibrium and multiple chaotic attractors. Nonlinear Dyn. 2015;81:585–605.
85. Li Y, Wang C, Chen H. A hyper-chaos-based image encryption algorithm using pixel-level permutation and bit-level permutation. Opt Lasers Eng. 2017;90:238–46.
86. Lu J, Guanrong C. A new chaotic attractor coined. Int J Bifurc Chaos. 2002;12(3):659–61.
87. Yuan H, Liu Y, Lin T, et al. A new parallel image cryptosystem based on 5D hyper-chaotic system. Signal Process Image Commun. 2017;52:87–96.
88. Gao T, Chen Z. A new image encryption algorithm based on hyper-chaos. Phys Lett A. 2008;372:394–400.
89. Liu C, Liu T, Liu L, Liu K. A new chaotic attractor. Chaos Solitons Fract. 2004;22(5):1031–8.
90. Vaidyanathan S, Volos C, Pham V. Hyperchaos, adaptive control and synchronization of a novel 5-D hyperchaotic system with three positive Lyapunov exponents and its SPICE implementation. Arch Control Sci. 2014;24(4):409–46.
91. Chai X, Gan Z, Yang K, et al. An image encryption algorithm based on the memristive hyperchaotic system, cellular automata and DNA sequence operations. Signal Process Image Commun. 2017;52:6–19.
92. Cang S, Qi G, Chen Z. A four-wing hyper-chaotic attractor and transient chaos generated from a new 4-D quadratic autonomous system. Nonlinear Dyn. 2010;59(3):515–27.
93. Peng ZW, Yu WX, Wang JN, et al. Dynamic analysis of seven-dimensional fractional-order chaotic system and its application in encrypted communication. J Ambient Intell Humaniz Comput. 2020. https://doi.org/10.1007/s12652-020-01896-1.
94. Murali P, Sankaradass V. An efficient space filling curve based image encryption. Multimed Tools Appl. 2019;78(2):2135–56.
95. Muthu JS, Paul AJ, Murali P. An efficient analyses of the behavior of one dimensional chaotic maps using 0–1 test and three state test. IEEE Recent Adv Intell Comput Syst. 2020;2020:125–30. https://doi.org/10.1109/RAICS51191.2020.9332470.
96. Muthu JS, Murali P. A new chaotic map with large chaotic band for a secured image cryptosystem. Opt Int J Light Electron Opt. 2021;242:242167300. https://doi.org/10.1016/j.ijleo.2021.167300.
97. Lalwani P, Banka H, Kumar C. BERA: a biogeography-based energy saving routing architecture for wireless sensor networks. Soft Comput. 2018;22:1651–67. https://doi.org/10.1007/s00500-016-2429-y.
98. Lalwani P, Das S, Banka H. CRHS: clustering and routing in wireless sensor networks using harmony search algorithm. Neural Comput Applic. 2018;30:639–59. https://doi.org/10.1007/s00521-016-2662-4.
99. Lalwani P, Banka H, Kumar C. CRWO: Clustering and routing in wireless sensor networks using optics inspired optimization. Peer Peer Netw Appl. 2017;10:453–71. https://doi.org/10.1007/s12083-016-0531-7.